Flooding duration and volume more important than peak discharge in explaining 18 years of gravel-cobble river change

By

ARIELLE A. GERVASI
THESIS

Submitted in partial satisfaction of the requirements for the degree of

MASTER OF SCIENCE

in

Hydrologic Sciences

in the

OFFICE OF GRADUATE STUDIES

of the

UNIVERSITY OF CALIFORNIA

DAVIS

Approved:

Gregory B. Pasternack, Chair

Amy E. East

Jonathan D. Herman

Committee in Charge

2021

Abstract

Floods play a critical role in geomorphic change, but whether peak magnitude, duration, volume, or frequency determines the resulting magnitude of erosion and deposition is a question often proposed in geomorphic effectiveness studies. This study investigated that question using digital elevation model differencing to compare and contrast three hydrologically distinct epochs of topographic change spanning 18 years in the 37-km gravel-cobble lower Yuba River (LYR) in northern California. Scour and fill were analyzed by volume at segment and geomorphic reach scales. Each epoch's hydrology was characterized using 15-minute and daily averaged flow to obtain distinct peak and recurrence, duration, and volume metrics. Epochs 1 (1999-2008) and 3 (2014-2017) were wet with large floods reaching 3,206 and 2,466 m^3/s, respectively, though of different flood durations. Epoch 2 (2008-2014) was a drought period with only four brief moderate floods (peak of 1,245 m^3/s). Total volumetric changes showed that major geomorphic response occurred primarily during large flood events; however, total scour and net export of sediment varied greatly, with 20 times more export in epoch 3 compared to epoch 1. The key finding was that greater peak discharge was not correlated with greater net and total erosion; differences were better explained by duration and volume above floodway-filling stage. This finding highlights the importance of considering flood duration and volume, along with peak, to assess flood magnitude in the context of flood management, frequency analysis, and resulting geomorphic changes.

Key words: fluvial geomorphology, DEM differencing, geomorphic effectiveness

Table of Contents

List of Figures

List of Tables

1 Introduction

What controls topographic change in a river? Fundamentally, change is measured as any positive or negative change in elevation (deposition and erosion, respectively) that occurs within the maximum boundaries of wetted extent over a designated period of time. Some broad physical controls on topographic change in fluvial systems include catchment-scale valley and channel topography (Montgomery, 1997; Peckham, 2003), sediment supply and bedload grain size (Carling 1988; Dietrich et al., 1989), vegetation roughness/distribution and woody debris (Lancaster et al, 2003; Abu-Aly et al., 2014), and hydrologic regime (Poff et al., 1997). Beyond these natural drivers, nearly all modern rivers change in response to human development including dams, channelization, mining, agriculture, or water extraction (e.g., Brown et al., 2017). Typical effects of damming, for example, include channel widening or contraction, coarsening or fining of bed substrate material, and channel incision, as well as altered hydrologic regime due to flow regulation (Williams & Wolman, 1984; Grant et al., 2003). Lane (1955) identified the balance between discharge characteristics and sediment supply as the key in determining channel incision or aggradation trajectory. More recently, East et al. (2018b) asserted that understanding channel response to sediment-supply disturbance is still one of the longest-standing problems in geomorphic process studies and is critical to understanding anthropogenic effects on watersheds.

Fluvial geomorphologists link ‘cause’ and ‘effect’ by quantifying the ability of hydrologic discharge to do work on a landscape through metrics such as shear stress (DuBoys, 1879), unit stream power (Bagnold, 1977), and geomorphic effectiveness (Wolman & Miller, 1960). Holding grain size and density constant, uniform channel dynamics equations dictate that higher peak flow leads to more erosion, as shear stress and total bed load transport scale proportionally with discharge. Conversely, geomorphic effectiveness studies have implicated flooding duration and

energy as the primary metrics that determine the magnitude of resulting topographic changes (Lisenby et al., 2016). The relative roles and importance of different discharge metrics are unclear. The overall goal of this study is to evaluate whether flooding peak flow, duration, or volume drives more topographic change in a gravel-cobble river setting, while accounting for other non-hydrologic or topographic influences within the study setting.

1.1 Topographic change processes in rivers

By measuring spatial patterns and temporal dynamics of erosion and deposition, fluvial geomorphologists infer topographic change mechanisms. Studies in fluvial geomorphology and morphodynamic theory have historically proposed, defined, and quantified mechanisms controlling change in response to topographic forcing or hydrologic events to explain why rivers change the way they do, with the ultimate prospect of predicting how rivers will change using morphodynamic models. Overall, fluvial topographic change processes (e.g., knickpoint migration, lateral channel migration, channel downcutting, floodplain aggradation) are governed by the interplay of hydrodynamic processes (e.g., particle trapping, eddying, backwatering) and the topographic structure controlling the river at various stages (**Figure 1**). Predictive morphodynamic models for unsteady, non-uniform flow conditions (such as those encountered in most rivers, in contrast with flume experiments) are progressing but exclude important processes and produce results with large uncertainties. Model advancements require more observational understanding to guide their progress (Kleinhans, 2010; Weber & Pasternack, 2017). Through repeat topographic surveys, the processes governing secular, temporal change versus self-maintenance of landforms in a river may be determined.

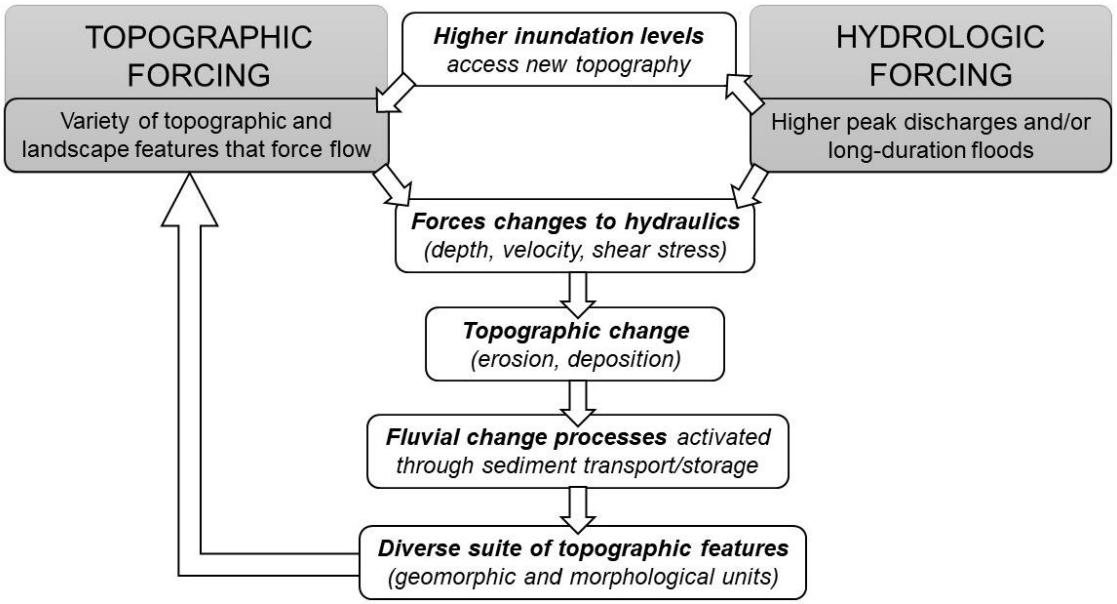

Figure 1. Conceptual diagram illustrating the interplay between topographic and hydrologic forcing in fluvial change processes. It should be noted that this diagram is focused on internal dynamics and excludes sediment supply input, which can further drive river form and topography.

1.2 Hydrologic regime significance

The concept of the hydrologic regime acknowledges the significance of timing; how flow is distributed and its variability through time can drastically alter the effect of a particular discharge (Costa & O'Connor, 1995; Lisenby et al., 2016). Hydrologic regime metrics – timing, magnitude, frequency, duration, and rate of change – may all affect geomorphic dynamics (Pickup, 1976). Antecedent hydrologic conditions and climatic shifts can create conditions that alter the effect of subsequent discharge events in complex fluvial systems (Gray et al., 2015a). Flood frequency analysis relies upon characterization of flow variation and is critical for effective floodplain and reservoir management (Bačová-Mitková & Onderka, 2010). This method uses the statistical distribution of particular flows throughout the historical record to predict the recurrence of particular discharges in order to plan for their arrival; for example, estimation of flood magnitudes corresponding to chosen flooding risks or failure of a structure is an important part of water management engineering practice (Bezak et al., 2014).

1.3 Geomorphic effectiveness

Fluvial geomorphologists quantify the ability of hydrology to do work on and change landscape topography through the concept of geomorphic effectiveness (Wolman & Miller, 1960). Typical hydrologic metrics implicated and quantified in the literature include discharge and recurrence interval, rainfall duration and intensity, shear stress, unit stream power, and total flood energy (Lisenby et al., 2016). Threshold discharges above which sediment may be entrained and erosional processes will occur are often determined on a site-scale basis with consideration for mean grain size, with significant thresholds including a river's dominant, effective, bankfull, and channel-forming discharges (Carling, 1988; Lenzi et al., 2006; Yochum, et al., 2017; East et al., 2018a).

In uniform flow conditions, shear stress and total bedload transport scale proportionally with discharge and dictate that a greater peak discharge will transport and erode more sediment. However, a review of geomorphic effectiveness studies by Lisenby, et al. (2016) concluded that flood energy is the best metric by which to quantify hydrologic 'cause' of geomorphic response. Under the geomorphic effectiveness model, flood archetypes have been defined using the flood energy metric (**Figure 2**). Floods that are long-lived, but with a low peak (**Figure 2C**), as well as floods of high peak, but short duration (**Figure 2A**) may cause little geomorphic change due to lack of energy generated above alluvial erosion threshold. Floods that have a high peak and long duration (**Figure 2B**) are predicted to be the most geomorphically effective floods, transporting large volumes of sediment (Costa and O'Connor, 1995).

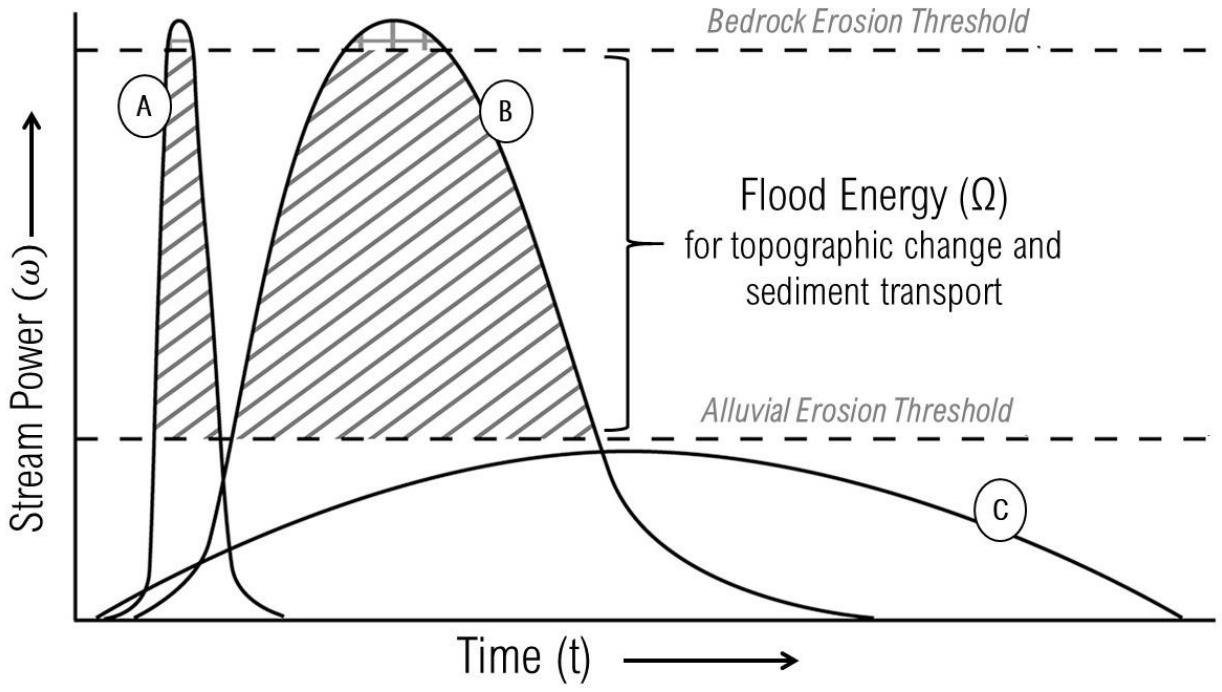

Figure 2. Relationship between stream power (ω in unit such as Watts/m^2) and flood energy (Ω in unit such as Joules) for sediment transport for three different flood archetypes. A) High peak, short duration flood. B) High peak, long duration flood. C) Low peak, long duration flood (reproduced from Lisenby et al. (2016), with permission from Wiley).

2 Study Objectives

Clearly, flood peak is an important component of the hydrologic regime, but just how significant is it in regard to geomorphic effect and topographic change when compared to flooding duration and energy, and the interplay of these hydrologic components? This study used digital elevation model (DEM) differencing with uncertainty analysis to quantify topographic changes at two spatial scales (segment and geomorphic reach), and then quantified specific hydrologic metrics to evaluate how topographic changes are driven by hydrologic and topographic controls independently, and in tandem. The study employed the multi-scalar, object-oriented framework from Pasternack and Wyrick (2016) to address questions related to where topographic changes are occurring over time (**Table 1**, Objective 1). Then, to address hydrologic controls, a novel framework was implemented to characterize the hydrologic regimes

for each study period beyond “drought” or “flood” designation; peak, volume, and duration metrics were chosen due to their relevance to geomorphic effectiveness. Five significant discharges and their inundation zones were chosen to represent thresholds (**Table 1**, Objective 2). After collecting and analyzing both topographic and hydrologic data, relationships between the topographic changes (scour, fill, and net) and the hydrologic metrics were explored to determine which hydrologic periods were more geomorphically effective, and answer the following overarching study questions:

1) What are the non-hydrologic topographic features and local influences that explain observed topographic changes?

2) Does greater peak flow lead to more erosion? If not, what other hydrologic metrics explain erosion and topographic changes?

Table 1. Study design.

Objective		Scale	Questions	Metric	Method
1-Topographic change scales and metrics across epochs 1-3	**A**	Segment	• Is the LYR net scour or net fill? • How was scour and fill distributed between in-channel and overbank regions?	Volume sediment (m^3)	• Measure total volume of scour and fill in the LYR. Scour – fill = net. • Stratify into in-channel ($\leq$113.26 m^3/s) and overbank ($>$113.26 m^3/s) regions and repeat.
	B	Reach	• What was the profile of fill/scour from upstream to downstream? • Which reaches were net sources or sinks of sediment?	Volume sediment (m^3, m^3/year)	• Stratify scour, fill, and net by geomorphic reach to create sediment budgets. • Net scour = source. Net fill = sink.
2-Characterize the hydrologic regimes through hydrologic metrics	**A**	15-minute	• What were the peak flows (year/epoch)? • What are the recurrence intervals for these peak events?	Peak (m^3/sec)	• Compile gage flow readings between 1999 and 2017 water years and find annual peaks. • Use Bulletin 17-B method in HEC-SSP to calculate recurrence intervals.
	B	15-minute, Daily	• What was the total discharge (year/epoch)? • What were the volumes of water discharged above significant inundation zones?	Volume water (m^3)	• Convert flow to volume and sum for each year using daily flow. • From the 15-minute gage flows, integrate the volume released above each inundation zone.
	C	15-minute	• What was the duration in days above the inundation zones?	Duration (days)	• Calculate the amount of time spent at or above each inundation zone discharge.

3 Study Site

The lower Yuba River of north central California was selected as the testbed river, because its topographic changes have been monitored systematically for three epochs during the period 1999-2017. The 37-km lower Yuba River (LYR) segment (**Figure 3**) is a single-thread channel (~ 20 emergent bars/islands at bankfull) with low sinuosity, high width-to-depth ratio, slight to no entrenchment, and eight distinct geomorphic reaches (Wyrick & Pasternack, 2012). Englebright Dam (**Figure 3**, panel 2) initiates the segment and is a 79-m high dam with a small water storage capacity that effectively blocks all sediment supply. The regulated river segment has a mean bed slope of 0.185% and a mean surface substrate diameter of 97 mm (i.e., small cobble). Daguerre Point Dam (DPD) is an 8-m high sediment barrier/irrigation diversion dam located at river kilometer (RKM) 17.8 upstream from the Feather River confluence. Its sediment storage capacity is full. Dry and Deer Creeks are gaged LYR tributaries upstream of DPD that are both dammed. Using the LYR 2006/2008 DEM, Wyrick and Pasternack (2012) delineated four lateral inundation zones (**Figure 3**, panel 3). The bankfull channel and floodway are delineated by discharges of 141.6 and 597.5 m^3/s, respectively.

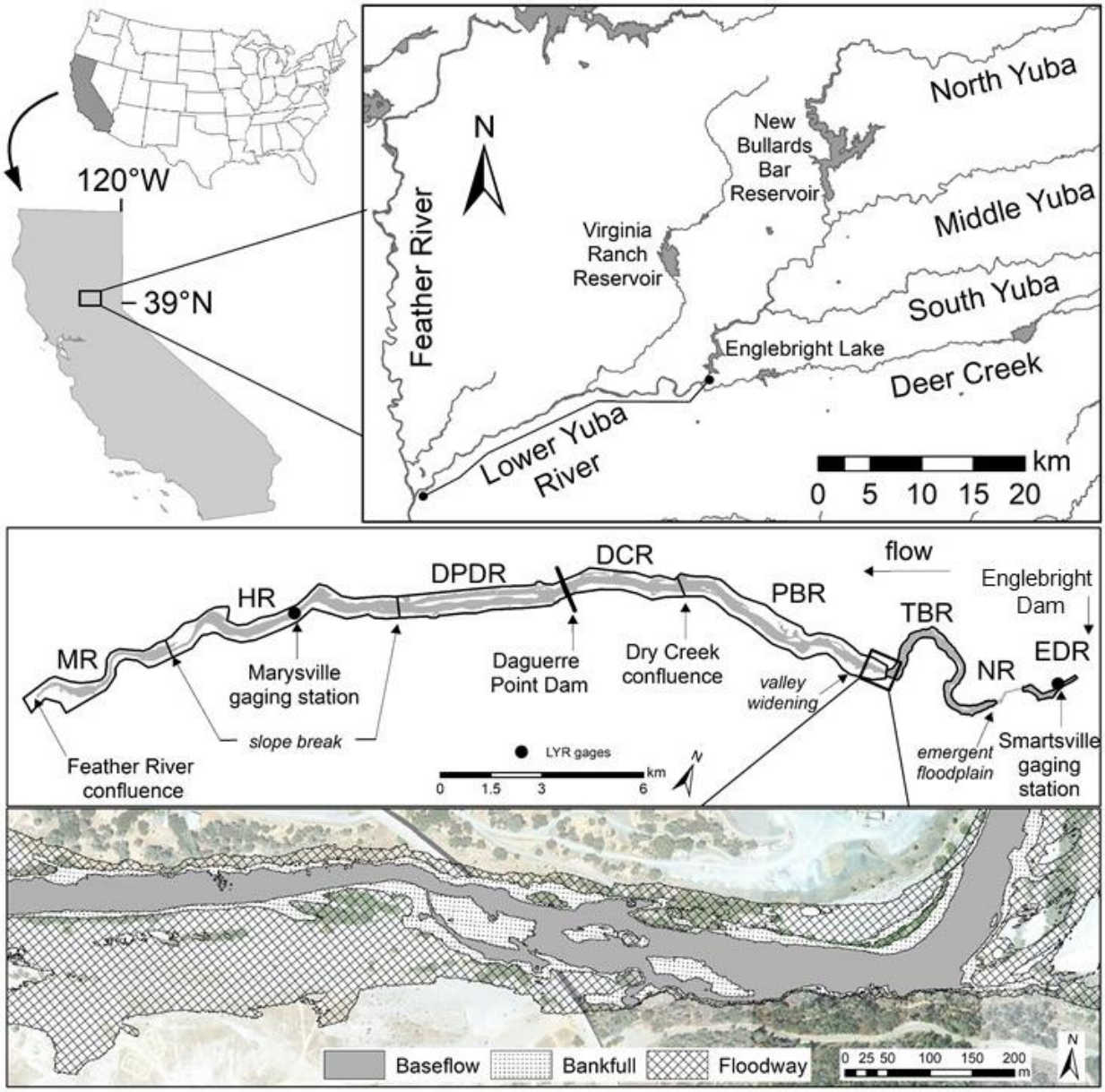

Figure 3. Location map showing the LYR and its eight geomorphic reaches, including key reach break factors and USGS gaging stations, Marysville and Smartsville. Reach acronyms: Marysville Reach (MR), Hallwood Reach (HR), Daguerre Point Dam Reach (DPDR), Dry Creek Reach (DCR), Parks Bar Reach (PBR), Timbuctoo Bend Reach (TBR), Narrows Reach (NR), and Englebright Dam Reach (EDR). Bottom panel: LYR inundation zones at baseflow (~ 18.5 m^3/s), bankfull (141.6 m^3/s), and floodway (597.5 m^3/s).

3.1 Topographic change history

Since the California Gold Rush there has been a 170-year history of dramatic geomorphic river changes in the Yuba River catchment and a subsequent need for monitoring these changes. Like many Sierra Nevada rivers, this one has historic and modern anthropogenic impacts, notably hydraulic and dredge-based gold mining, deforestation, agriculture, river training, and flow regulation. The Yuba River experienced extreme sedimentation and sediment transport after hydraulic mining operations ended—the California Debris Commission estimated that the valley accumulated ~ 200 million m^3 of mining sediment in the late 19^{th} century (Gilbert, 1917; Adler, 1980). During the early 20th century, high sediment loads overwhelmed the transport capacity of valley channels and caused major geomorphic adjustments such as channel aggradation and avulsions (Adler, 1980; James et al., 2009). Englebright Dam was installed in 1940 to block all bedload and most suspended load from entering the LYR, thereby promoting some downstream geomorphic recovery—even after 80 years, recovery continues (James, 2005).

3.2 Hydrology

The Yuba watershed's climate involves little to no precipitation June through September and then a wet season late November to May with precipitation of ~ 500-2000 mm depending on elevation and aspect. Wet-season floods are often generated by narrow-banded atmospheric rivers that deliver localized, intense, high-magnitude precipitation (Ralph et al., 2006; Dettinger, 2011). Extreme precipitation events that occur remarkably regularly with a periodicity of ~ 10 years (Guinn, 1890) deliver large quantities of warm rainfall onto snow-packed mountain slopes. Flow analysis statistics on the western coast of the U.S. reveal that these interannual to decadal cycles between dry and wet periods are caused by El Niño Southern Oscillation (ENSO) cycles (Gray et al., 2015b).

The LYR's flow regime is highly dynamic. Two of the major tributaries contributing to the LYR (Dry and Deer Creeks) do not have large water supply dams and cannot abate floods. Although the river is partially regulated through New Bullards Bar on the North Yuba and Englebright Dam on the mainstem, the latter is kept nearly full. Flows greater than bankfull discharge overtop the ogee-crested dam or pass through two smaller (12,000 kW and 50 mW) powerhouses located immediately downstream and are rapidly delivered to the lower Yuba River segment with only mild attenuation.

The key hydrological point for this study is that the 1999-2017 period encompasses two extreme, wet period flood events, creating the unique ability to not only contrast large versus small flood regimes, but also two large flood regimes. Conditions were average to dry 1999-2005, because the previous large flood event happened in 1997 before systemic topographic surveying got underway. A large flood (peak of 3,207 m^3/s; 23-year recurrence) occurred in the 2006 water year, but then from 2012-2016 the entire western US experienced a severe drought (East et al., 2018a; Swain et al., 2018). The next large flood event occurred during the 2017 winter (peak of 2,466 m^3/s; 13-year recurrence), which became one of the wettest on record for the western US, with integrated vapor transport estimated at three standard deviations above the mean quantity for the California coast (Gershunov et al., 2017; East et al., 2018b).

4 Methods

4.1 Temporal scale and topographic surveys

The LYR's topography has been closely monitored over the 18-year period between 1999 and 2017. Four high-resolution DEMs of the river bed and valley bottom provided topographic snapshots from the following years: (i) 1999, collected using aerial photogrammetry and single beam echosounding; (ii) 2006/2008, collected using airborne near-infrared LiDAR,

single beam echosounding tied to RTK GPS, and ground surveys; (iii) 2014, collected using primarily airborne LiDAR with both near-infrared and green lasers, as well as multibeam and single beam echosounding tied to RTK GPS, and ground surveys; (iv) 2017, collected with the same methods as in 2014. The date for the second DEM is combined as 2006/2008 because Timbuctoo Bend was mapped in 2006 and then the rest of the river (excluding the Narrows Reach that was left unsurveyed) was predominantly surveyed in 2008.

An epoch is the time period between two topo-bathymetric surveys. In this study there are three epochs: (i) epoch 1 is the 7-9 year period between 1999 and 2006/2008 (Pasternack and Wyrick, 2016); (ii) epoch 2 spans 6-8 years between 2006/2008 and 2014 (Weber and Pasternack, 2017); (iii) epoch 3 is the 3-year period between 2014 and 2017, with this study introducing this latest set of topographic change results. Epoch 3 is short because a large flood in 2017 warranted new mapping.

4.2 DEM differencing and topographic change detection

The differencing of sequential DEMs with an accounting of uncertainty creates three DEMs of Difference (DoDs) for the three change epochs from the four input DEMs for the LYR. Pre-existing peer-reviewed DoD rasters were used from Carley et al. (2012) for epoch 1 and Weber and Pasternack (2017) for epoch 2. Epoch 3 is the latest period. Its DoD raster was produced using the same data collection and topographic change detection (TCD) procedure methods as in Weber and Pasternack (2017). The TCD procedure used herein for the 2014-2017 data provided a spatially explicit uncertainty raster (Level of Detection raster) to account for and combine error from multiple sources including land cover type (vegetation, water, or bare earth), topographic variability due to slope, DEM interpolation, and sampling point density. Vertical error incorporated into the Level of Detection raster ranged from 0.02 to 6.02 meters across the entire study site, and was log-normally distributed, with error concentrated at the

lower end of the values. The mean error was 0.16 m, with a median of 0.10 m, skewness of 1.97, and a standard deviation of 0.17 meters. The Level of Detection raster containing the estimated vertical error in elevation values was subtracted from the raw difference between 2014 and 2017 DEMs prior to topographic change analysis, so that the reported elevational change in the resultant DoDs is within a 95% confidence interval.

4.3 Topographic change framework

Topographic changes were analyzed at segment (entire LYR), geomorphic reach, and morphological unit scales to isolate patterns of change to address different scientific questions (Pasternack & Wyrick, 2016). The questions raised in this study only involve the first two spatial scales, because these were the only scales that could be applied uniformly across all three study periods. In-channel versus overbank lateral inundation zonation is a stratification of the segment-scale data. Ideally a boundary for the estimated bankfull discharge (141.6 m^3/s) would be available for all survey dates, but the only available wetted extent for 1999 was 109 m^3/s, so the closest available extent to that for the other epochs (from two-dimensional hydrodynamic modeling of a steady 113.26 m^3/s) was used to delineate the channel regions for all epochs instead, as was done in previous work (Pasternack & Wyrick, 2016). Areas outside this near-bankfull boundary are referred to as overbank regions.

This study analyzed topographic change by scale using area (m^2, %), volume (m^3, m^3/year), and sediment depth (mm/year) metrics, with extra area, volume, and depth results reported in supplementary materials. Due to different durations and survey timing in epochs 1, 2, and 3, scour and fill volumetric results were originally normalized by year (m^3/year) for direct comparison on a time-free basis. However, the volumetric changes reflect not only differences in driving process, but also how long there was for change to occur, which varied from 3 to 9 years depending on the reach and epoch. While annual rates represent intensity of changes,

total volumetric flux (m^3) represents overall geomorphic effectiveness (Lisenby et al., 2016) over the entire epoch.

To calculate volumetric sediment budgets of scour and fill using DoD rasters, the areal distributions of scour and fill were multiplied by the mean change in elevation that occurred within the spatial scale of interest using the Zonal Statistics tool in ArcGIS 10.5. Because uncertainty was already accounted for in producing DoD rasters, no further steps are required to assess volumetric uncertainty (Pasternack and Wyrick, 2016). The LYR sediment budget is greatly simplified due to the presence of upstream dams on the mainstem and tributaries, which block nearly all sediment load. As a result, net influx of sediment into the LYR is assumed to be zero.

4.4 Hydrologic metric framework

For each epoch, the following metrics were collected: peak discharge and duration and volume above significant discharge thresholds in the river. Discharge (Q) in m^3/s is used in place of unit stream power (ω in Watts/m^2) from the geomorphic effectiveness metrics (**Figure 2**), because these terms are equivalent when controlling for fluid density (ρ), gravitational acceleration (g), slope (S), and channel width (w), by considering the entire river as one unit at the segment scale (Equation *[1]*). Volume (V), in m^3, can then be substituted for flood energy (Ω in Joules) because it is simply the integration of the stream power, or discharge (Q) in this study, over a period of time (dt) (Equation *[2]*).

The major lateral inundation zones of the river previously delineated using the LYR 2006/2008 DEM by Wyrick and Pasternack (2012) were employed to represent discharge thresholds (eg., **Figure 3**, bottom panel). These thresholds set time intervals over which volume was integrated. These discharges for the LYR include: bankfull (141.6 m^3/s), 2x bankfull (283.2 m^3/s), floodway (597.5 m^3/s, also termed the “floodplain-filling flow”), 6x bankfull (849.5 m^3/s),

and flood-prone area (1,195 m^3/s). To produce the most precise metrics, 15-minute flow data was used to calculate peak, duration, and volume above thresholds, while daily averaged flow was used only to calculate annual volumes. Because 2008 is the survey year for the majority of the LYR in the second DEM (the lower 5 reaches below TBR), the hydrologic analysis uses the 2008 water year as end year for epoch 1 (1999-2008) and start year for epoch 2 (2008-2014).

$$\omega = \frac{\rho g Q S}{w} \rightarrow Q \quad [1]$$

$$\Omega = \int \omega \, dt \rightarrow V = \int Q \, dt \quad [2]$$

Annual water year statistics and metrics were obtained from two USGS flow gages: Smartsville (#11418000) and Marysville (#11421000) (**Figure 3**). Recurrence intervals for key peak discharges were calculated from the Smartsville flow data on a water year basis (October to September) using the Bulletin 17-B method, implemented in HEC-SSP. All other hydrologic metrics were derived from flow readings from the Marysville gage, which includes discharge contributions from the Dry and Deer Creek tributaries, but excludes seasonal diversions for irrigation and other uses.

5 Results

5.1 Objective 1: Topographic changes

5.1.1 Part A – Segment scale

In epoch 1, a small net of 0.06 x 10^6 m^3 of sediment was exported out of the LYR as large volumes of scour material (-2.52 x 10^6 m^3) (all scour values reported with a negative symbol) re-deposited downstream within the river (2.46 x 10^6 m^3) (**Figure 4**). Net export volume increased to 0.14 x 10^6 m^3 in the drought period of epoch 2, resulting from -0.64 x 10^6 m^3 of scour and only 0.50 x 10^6 m^3 of deposition. Over three years in epoch 3, the LYR experienced more scour than epoch 1 and simultaneously experienced less re-deposition (-3.39 x 10^6 m^3 and

2.03 x 10^6 m^3 respectively). This resulted in a net erosional export of 1.37 x 10^6 m^3, > 20 times greater than the export over the 9 years of the first epoch.

A comparison of channel change between the channel and overbank areas found that they were net fill and net scour, respectively, for all epochs (**Figure 5**). This is an opposite outcome from the expectation for regulated rivers. However, the distribution of scour and fill within and between in-channel and overbank regions was unique in each epoch. Epoch 1 showed the most balance between scour and fill volumes between regions and the most re-deposition of sediment in the overbank (1.84 x 10^6 m^3) of any epoch. In epoch 2, the overbank was less active, with a greater percentage of scour and re-deposition occurring in the in-channel regions; it experienced the lowest net fill in the channel region (0.12 x 10^6 m^3) and lowest percent overbank fill of any epoch. Epoch 3 had the greatest in-channel fill (1.25 x 10^6 m^3) and overbank scour (-2.67 x 10^6 m^3) of any epoch. In all cases, the majority of segment scale scour came from the overbank region, but in both epochs 1 and 3, the overbank contributed a majority, about 80%, of the total scour volume.

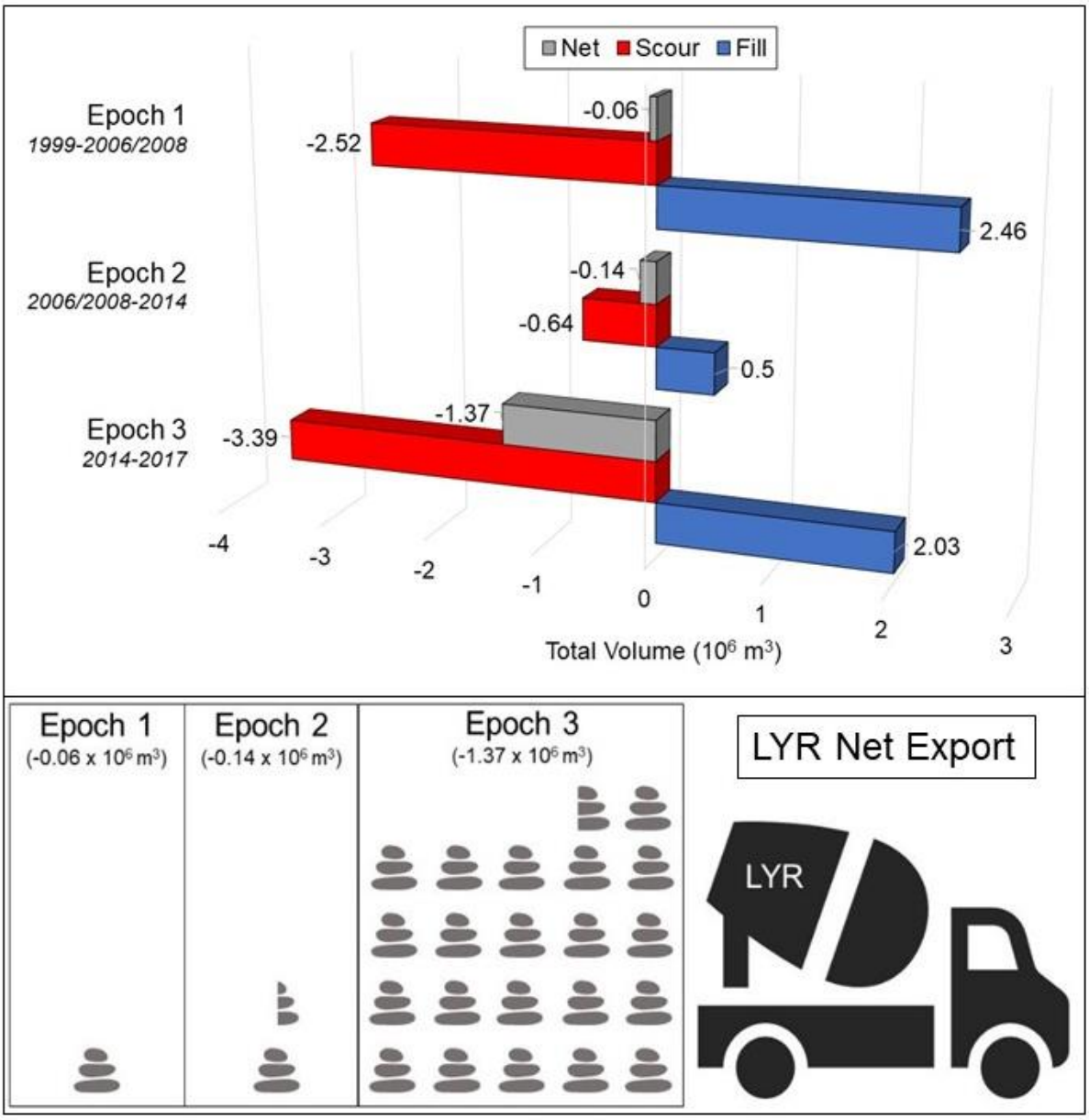

Figure 4. Total volume of scour, fill, and net in 10^6 m^3.

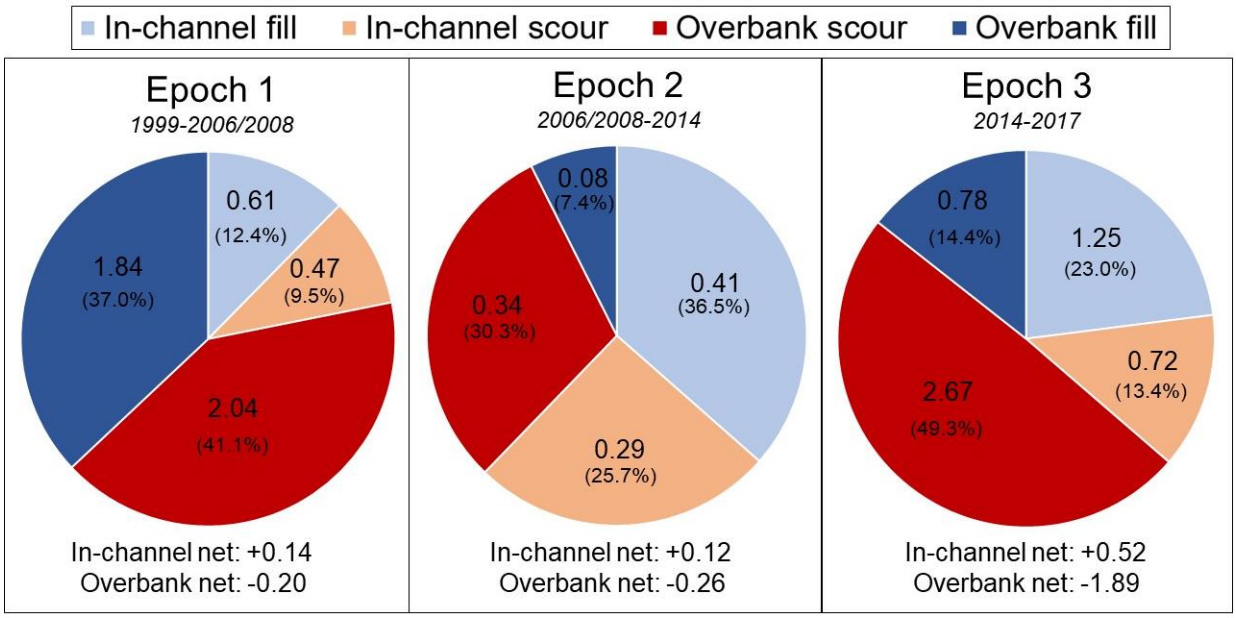

Figure 5. Total volumetric changes in 10^6 m^3, stratified into in-channel and overbank regions.

5.1.2 Part B – Reach scale

TBR, at the top of the LYR segment, remained net scour in all epochs (**Figure 6**). PBR varied between net depositional in epoch 1 and net erosional in epochs 2 and 3, due to relatively balanced scour and re-depositional processes. Despite being upstream of a dam and downstream of a tributary confluence supplying some sediment, DCR was consistently net erosional across epochs and was the only reach that experienced greater scour volume in epoch 1 (-62.74 x 10^4 m^3) than in epoch 3 (-49.72 x 10^4 m^3). Below DPD, DPDR exhibited an interesting pattern in that it was the most net depositional reach in epoch 1, the most net erosional reach in epoch 2, and the only net depositional reach in epoch 3. Next downstream, HR shifted from strongly net depositional in epoch 1, to nearly net neutral in epoch 2, and then experienced the greatest scour volume of any reach over all epochs at -76.08 x 10^4 m^3 of scour in epoch 3, making it the most net erosional reach in that epoch. Lastly, MR, which connects to the Feather River confluence, experienced scour and fill patterns similar to PBR, shifting gradually from a net depositional reach in epoch 1 to net erosional in epochs 2 and 3.

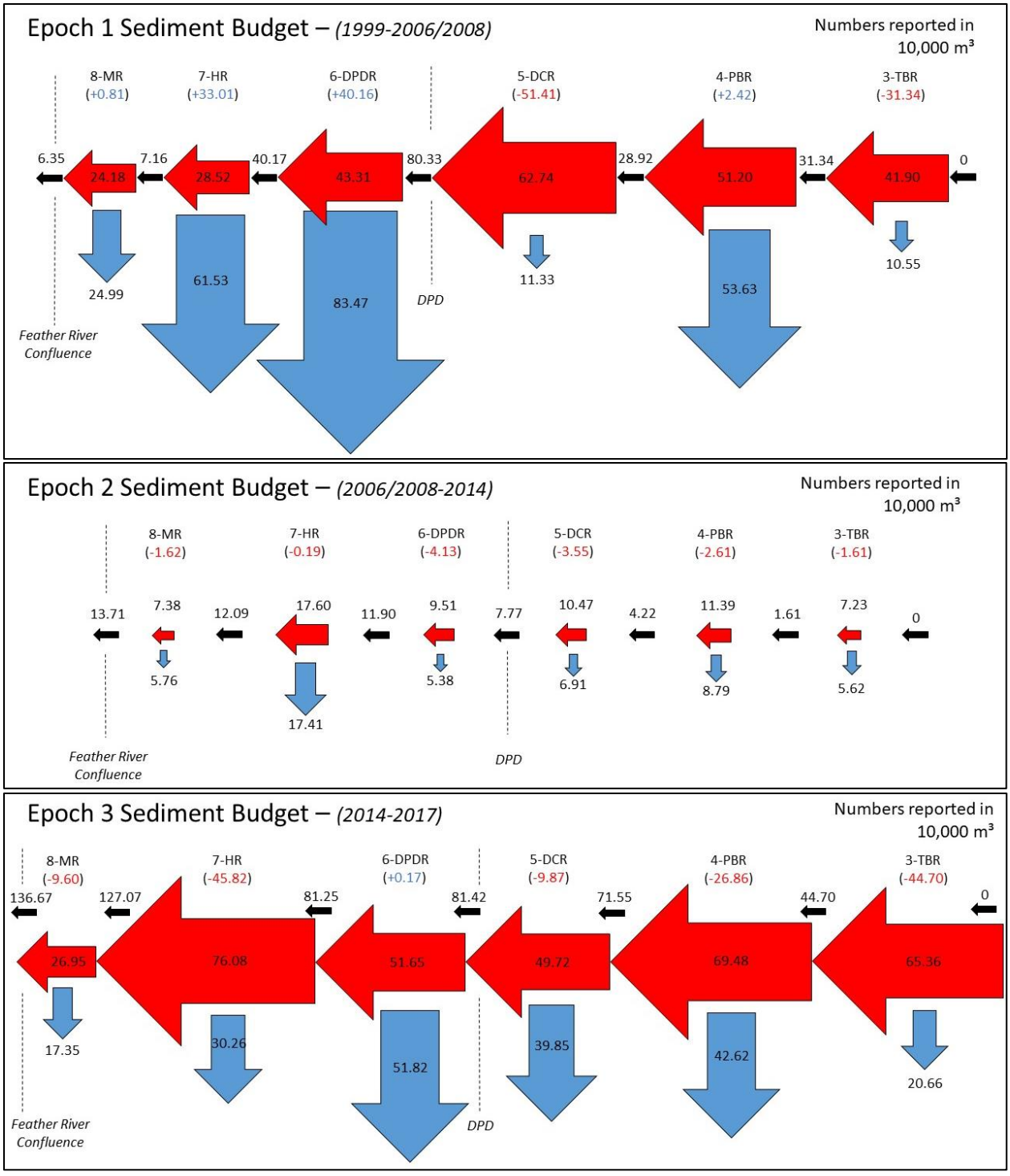

Figure 6. Total volume of sediment scoured (red horizontal arrows) or re-deposited (blue vertical arrows) in each reach, in 10^4 m³ with sizes scaled proportionally to volume. Horizontal arrows point in direction of flow. Numbers in parentheses indicate net for each reach. Black arrows indicate net transport between reaches.

Annualized results represent the total volumes divided by the number of years between DEM surveys, in order to standardize the results and compare the relative intensities of scour and re-deposition in each epoch (**Figure 7**). In epoch 3, HR experienced the greatest scour rate of any reach at 25.36 x 10^4 m^3/year of scour. After net changes were taken into account at each reach moving from upstream to downstream, the annualized rate of sediment export out of the LYR indicated an increase in export rate between the flood and drought periods of epoch 1 and 2, from 1.70 x 10^4 m^3/year to 2.22 x 10^4 m^3/year, an increase of only 30%. The next epoch, epoch 3, saw a net export rate of 45.56 x 10^4 m^3/year, 20 times greater than the export rate of epoch 2 and 25.8 times the export rate of epoch 1.

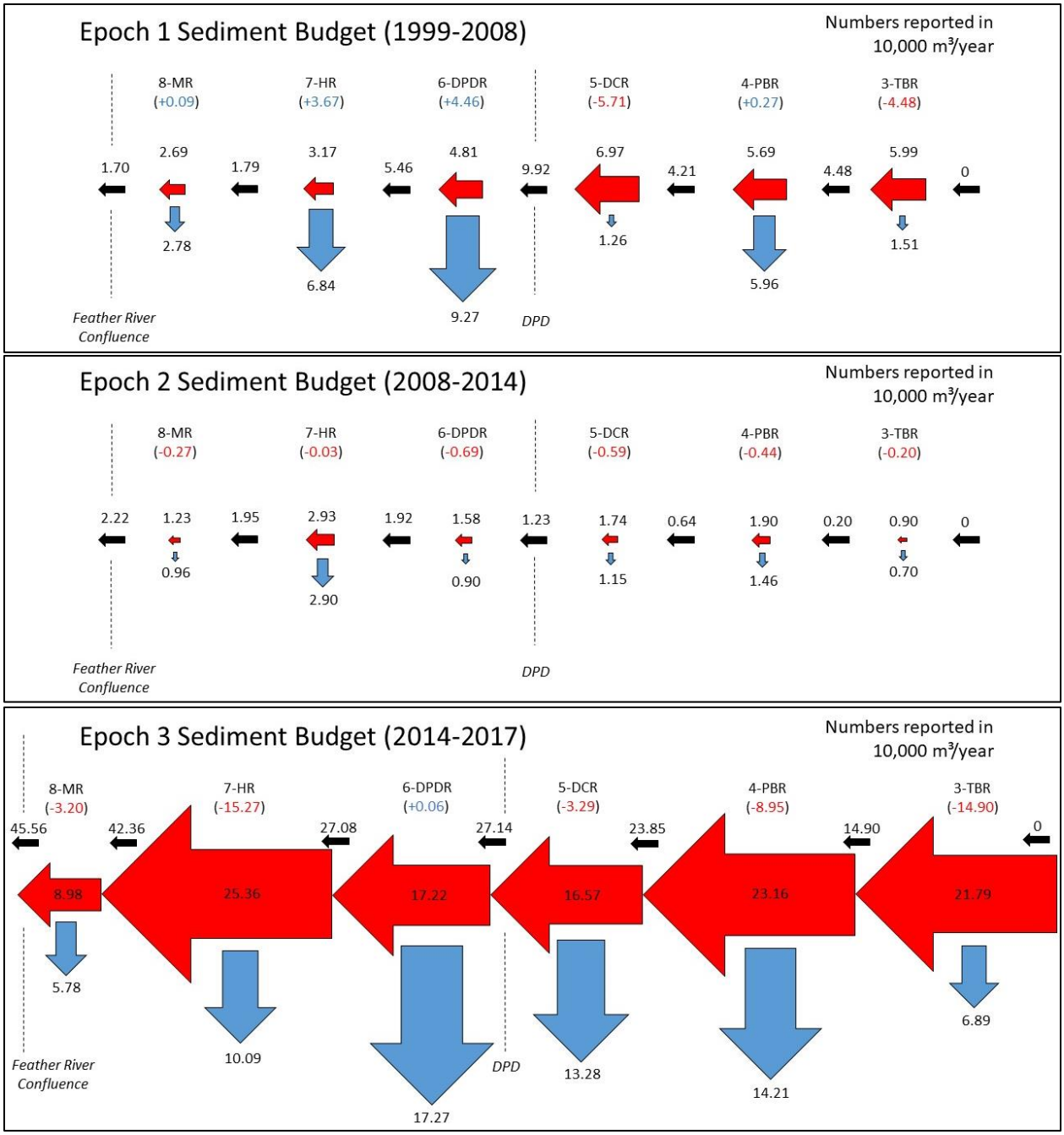

Figure 7. Annualized volumetric rates of sediment scoured (red horizontal arrows) or re-deposited (blue vertical arrows) in each reach, in 10^4 m³ with sizes scaled proportionally to volume. Horizontal arrows point in direction of flow. Numbers in parentheses indicate net for each reach. Black arrows indicate net transport between reaches.

5.2 Objective 2: Hydrologic metrics

5.2.1 Part A - Peak

Epoch 1, the longest epoch in the study, experienced the highest intensity flood (instantaneous discharge of 3,207 m^3/s in the 2006 water year), with a moderate flood the previous year and again in the following spring (**Figure 8**, **Table 2**). That peak event corresponds to a 23-year event and 22.6 times bankfull discharge. Epoch 2 was dry yet still had four floods filling the floodway (597.5 m^3/s), ranging from 875 to a peak of 1,245 m^3/s instantaneous flow in 2013. These flows correspond to ~ 3–5-year recurrence interval events and 6–9 times bankfull discharge. The maximum instantaneous discharge for epoch 3 was 2,466 m^3/s (January 2017), corresponding to a 13-year recurrence interval. This peak was ~ 25% less than that in epoch 1.

Table 2. Summary of water year statistics (epoch 2 shaded). Discharge data from daily average and 15-minute flow data from Marysville gage. Water year begins October 1st of the year prior to year indicated.

Water year	Instant. peak (m^3/s)	Daily avg. peak (m^3/s)	Annual avg. vol. (10^6 m^3/y)
2000	642.03	608.81	1,779
2001	63.49	55.78	697
2002	149.26	142.72	1,241
2003	236.25	231.07	1,829
2004	418.89	345.47	1,355
2005	1,480.12	1,228.95	1,830
2006	3,206.60	2,384.28	4,794
2007	374.97	283.17	901
2008	138.19	130.26	819
2009	566.34	356.79	1,242
2010	189.58	181.23	1,419
2011	874.99	761.72	3,838
2012	961.07	603.15	1,366
2013	1,245.94	628.63	1,272
2014	217.76	178.11	614
2015	195.00	147.53	527
2016	612.00	877.82	1,748
2017	2,466.00	2,217.21	6,288
Epoch 1	3,206.60	2,384.28	1,694
Epoch 2	1,245.94	761.72	1,625
Epoch 3	2,466.00	2,217.21	2,854

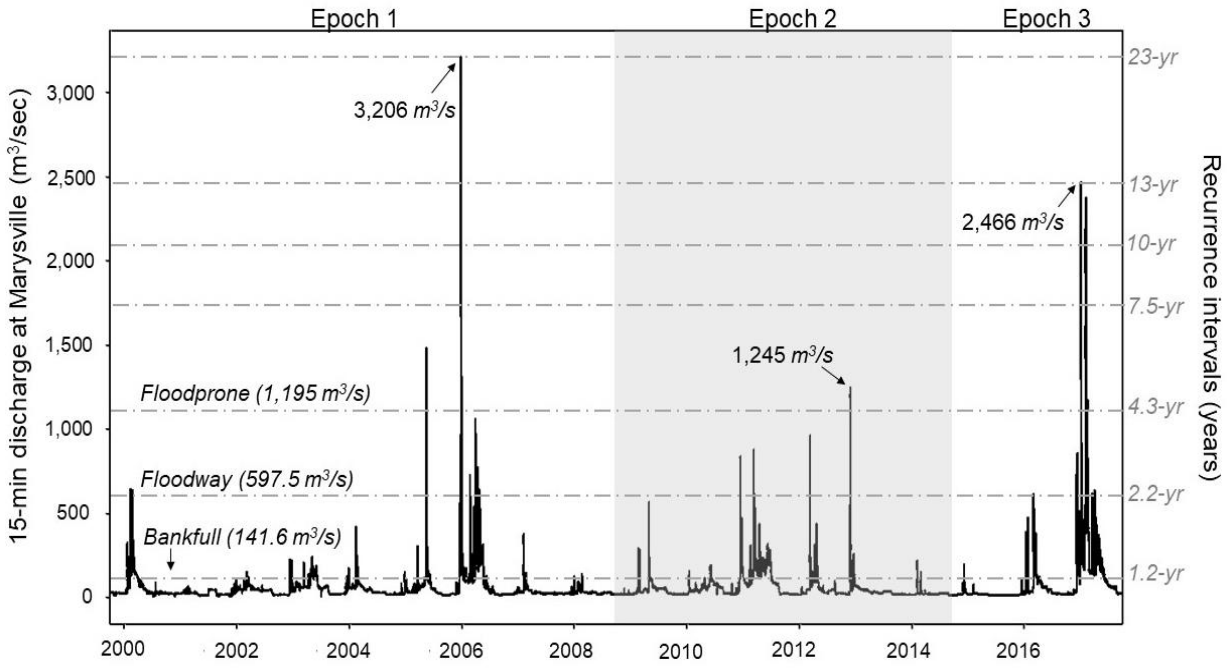

Figure 8. Hydrograph of 15-minute discharge across survey epoch 1 (Oct 1st 1999-Sept 30th 2008), epoch 2 (shaded, Oct 1st 2008-Sept 30th 2014), and epoch 3 (Oct 1st 2014-Sept 30th 2017). Recurrence intervals listed on right axis.

5.2.2 Part B - Volume

To calculate annual volumes released, daily average flows were summed for each water year (**Table 2**, last column). The 2017 water year resulted in the greatest annual volume at 6.29 x 10^9 m^3 of water. The 2006 water year in epoch 1 experienced the second highest volume at 4.79 x 10^9 m^3 and the third highest volume year was in 2011, during epoch 2.

For each epoch, the 15-minute flow data was used to calculate the volume of water that was released above five significant inundation zones (**Figure 9**, top panel). Epoch 1 experienced greater volumes of water above all thresholds relative to epoch 2. The volume of discharge above all thresholds was consistently higher in epoch 3 compared to the first two epochs. Notably, the discharge released above the three highest inundation zones (floodway, six times bankfull, and flood-prone) in epoch 3 was typically twice the volume released over the same threshold during epoch 1.

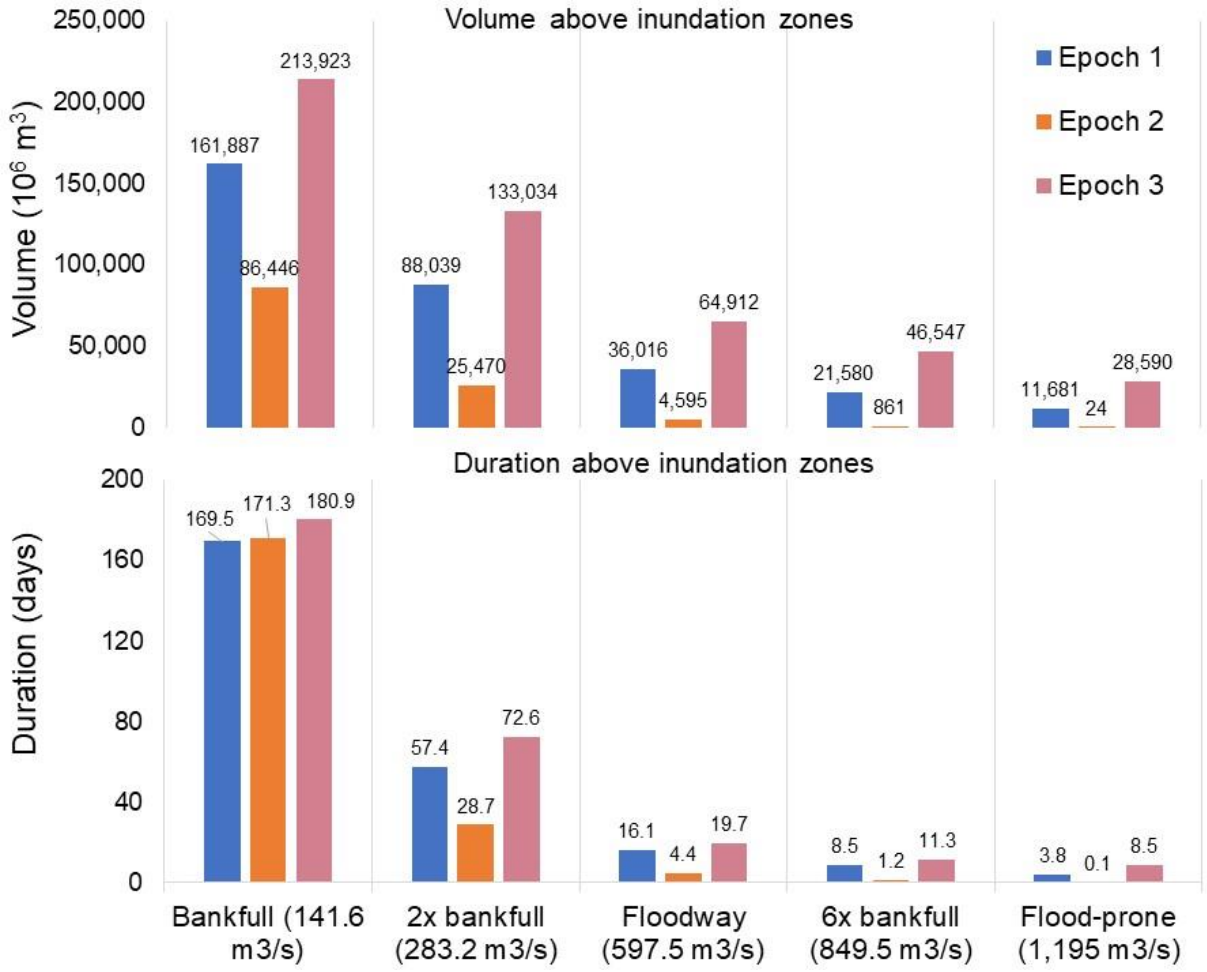

Figure 9. Volume and duration analysis in the LYR using 15-minute flow data from Marysville gage.

5.2.3 Part C - Duration

Duration analysis revealed that each epoch spent nearly the same amount of time at or above the bankfull stage (**Figure 9**, bottom panel), although in epoch 2 this did not correspond with a significant increase in volume (**Figure 9**, top panel). Epoch 1 spent 169.5 days above bankfull, epoch 2 spent 171.3 days above bankfull, while epoch 3 spent the most time above bankfull at 180.9 days. Beyond this threshold, differences in duration at 2x bankfull and above are more distinct across epochs. As with volume, epoch 3 experienced the longest duration

above all key inundation zones despite being the shortest period, and spent more than twice as many days above flood-prone relative to epoch 1.

Comparing the hydrographs for flood epochs 1 and 3 (**Figure 10**) highlights why epoch 3 experienced greater discharge volumes and durations, especially at the higher flood stages, relative to epoch 1. Epoch 3 experienced two nearly equivalent flood peaks in January and February of the 2017 water year, with sustained flood discharge through the month of February, whereas epoch 1 experienced only one peak flood event in the 2006 water year.

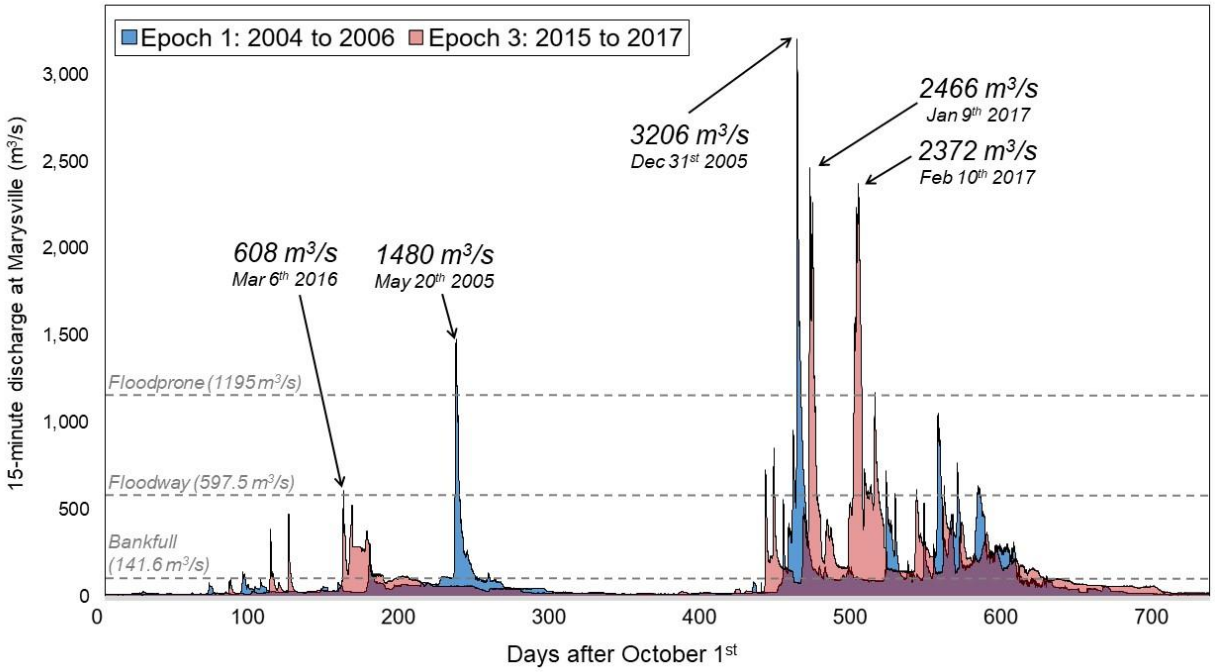

Figure 10. Hydrograph with two example years from epochs 1 (blue) and 3 (red).

6 Discussion

6.1 Study Question 1: Topographic features and internal dynamism

First, patterns in topographic change across the study epochs are explored, with a focus on topographic drivers, historic impacts, and local reach scale behavior. The LYR is strongly

influenced not only by stage-dependent topography, creating naturally variable channel depth and width, but its topography is also influenced by dams, historic hydraulic mining, levees, training berms, and natural terraces. Downstream of DPD, the valley has a wide floodplain and low slope gradient, but exhibits stage-dependent expansions and constrictions (Pasternack et al., 2018) creating a highly variable environment in regards to geomorphic response. By using the scale-based approach to analyzing topographic changes, patterns emerged in scour and re-deposition at the segment and geomorphic reach scales with implications for the topographic drivers controlling the underlying processes.

6.1.1 A non-incising channel and net scour system

Typically for a regulated river, one expects to see that dams cause in-channel incision, entrenchment, and disconnection between channel and floodplain (Williams and Wolman, 1984; Grant et al., 2003). However, the opposite appears to be the case for the LYR. As the channel migrates or avulses from its initial location to its final location at the end of the epoch, it tends to fill in its old channel while scouring through the banks and cutting new pathways over floodplains. There are several topographically driven explanations for lack of in-channel incision. First, the bed of the LYR is armored and consists of coarse gravel-cobble, but the steep (often unconsolidated) banks, levees, and mining tailings along the lateral edges are composed of fine gravels and sands (Wyrick & Pasternack, 2015). These finer sediments would be preferentially scoured over coarser sediments along the bed (Dietrich et al., 1989) and James (2005). Mining tailings indeed exhibited the third highest scour volume epoch 3 within MU analysis (see Supplemental Materials). However, this alone does not explain the erosive nature of the epoch 3 flood event. While steep surfaces like tailings and banks may only be erosional given their shape, flat surfaces like floodplains and terraces may be both erosional and depositional. The epoch 3 event yielded more balance between net erosion of flat surfaces (whether by lateral or vertical dynamics) and net erosion of tailings, with highest preference towards flat terrace and

floodplain surfaces. Therefore, the coarse gravel-cobble bed load is often not the subject of transport. Furthermore, the valley floor stores ~200 million cubic meters of hydraulic-mining alluvium (Gilbert, 1917; James et al., 2005), but between 1999 and 2017, 1.57 x 10^6 m^3 of sediment was exported from the LYR, which is only 0.78% of that amount. An excess of remnant mining sediments in the LYR may provide an internal accessible sediment load in the absence of external supply.

The LYR overbank (as well as the channel + overbank) was net scour in all epochs regardless of hydrologic regime. Englebright Dam was specifically designed to block sediment and both gaged tributaries (Dry and Deer Creek) downstream of the dam are themselves dammed. Therefore, this is a feasible result under the assumption that the channel receives no significant external sediment supply input. However, the immense internal supply from long-term storage from late 19th and early 20th century mining as well as observed re-mobilization of tailings sediment (James, 2005) makes it unsurprising to observe that the LYR is a consistent sediment exporter. The LYR's unique history and topographic influences must be taken into consideration when applying existing concepts of geomorphic response to explain the channel and overbank dynamics.

6.1.2 Reach scale influences

DPDR was the only reach to remain net fill in both flood regimes, but was net erosional in a drought period. Review of validated 2D hydrodynamic model results used for river management (**Figure 11**) confirm that flood-stage flows initiate channel expansion; at lower discharge, erosive forces are focused in the channel and on banks but after water spills onto the floodplain, channel velocity declines as patches of peak velocity shift onto the floodplain (Abu-Aly et al., 2014). This pattern may rely upon DPDR's ability to access the large Daguerre alley side channel (**Figure 11**) as the key topographic component that allows it to remain a sediment sink during flood regimes.

TBR and DCR were the only two reaches to remain the same (net scour) in all epochs regardless of hydrologic regime. Therefore, they may be driven more by topographic features than hydrology. Likely their proximity to dams “fixes” their roles, with TBR beginning with little sediment supply and DCR ending at a dam imposing a base level. TBR, in addition, is in a constricted valley within the Sierra foothills above the start of the alluvial fan (**Figure 3**) and may experience increased erosion as an effect of two processes. First, it receives sediment-starved “hungry water” (Kondolf, 1997), so it can scour from upstream to downstream to pick up sediment supply. However, there is no indication of a reduced slope at the head of TBR, so this would have a limited distance of downstream effect. Second, upstream migratory waves of channel adjustments are thought to have occurred (Carley et al., 2012) in response to an over-steep longitudinal bed-elevation profile (associated with hydraulic mining valley fill and evacuation history) relative to the equilibrium slope sustainable in light of the base level imposed by Daguerre Point Dam.

PBR, HR, and MR were all reaches that changed over time, from sediment sinks in epoch 1 to sediment sources in epochs 2 and 3, indicating factors that changed over time related to topographic dynamics as well as hydrology. Interestingly, these are also the reaches that are separated from a dam by at least one reach indicating lack of dam influence. The most clear example of a sequence of events where topographic forcing and hydrologic forcing interacted to produce a new topographic change outcome is illustrated in HR, where a terrace collapsed in epoch 3. While the valley and floodplains are generally wider downstream of DPD, constrictions exist at bends and the onset of levees. Topographic features are highly stage-dependent and constrictions are exacerbated at higher flows. As areas upstream collect more water and expand into the floodplain, nozzles form downstream as large volumes of water are forced to quickly flow through the constriction creating concentrated areas of high velocity and shear stress that easily mobilize sediment and promote erosion (Pasternack et al., 2018) (e.g., **Figure**

11). The major terrace erosion in HR was exactly at one such abrupt constriction downstream of DPDR. Aerial imagery revealed that the river began scouring into the sharp, constricting bend during epoch 2, setting the stage for the flood-driven collapse in epoch 3 (**Figure 12**). The terrace collapse accounted for 9.8% of the entire volume of sediment eroded downstream of DPD in epoch 3.

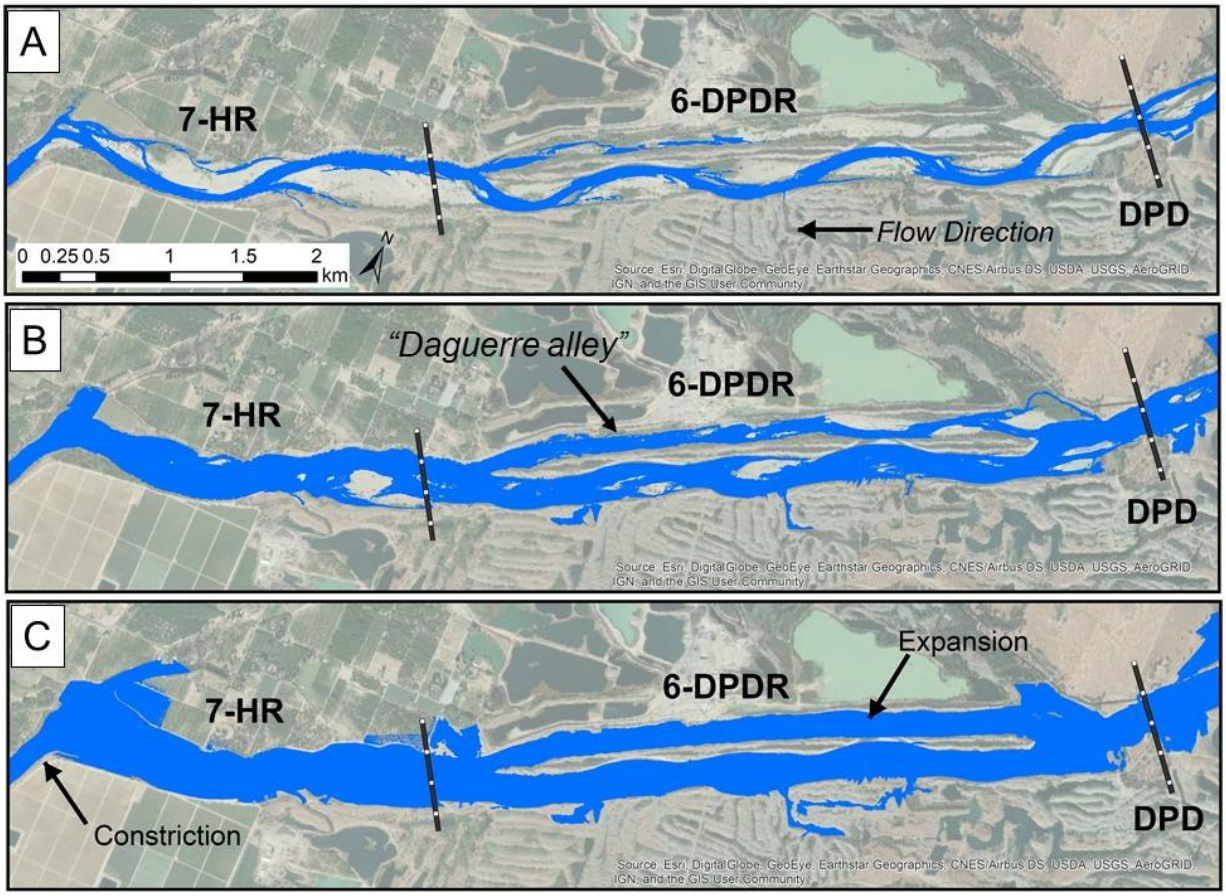

Figure 11. Wetted extents generated using a 2D hydrodynamic model with the 2014 topography. A) Bankfull (141.6 m^3/s). B) Floodway (597.5 m^3/s). C) Epoch 1 peak daily averaged flow (2,389 m^3/s).

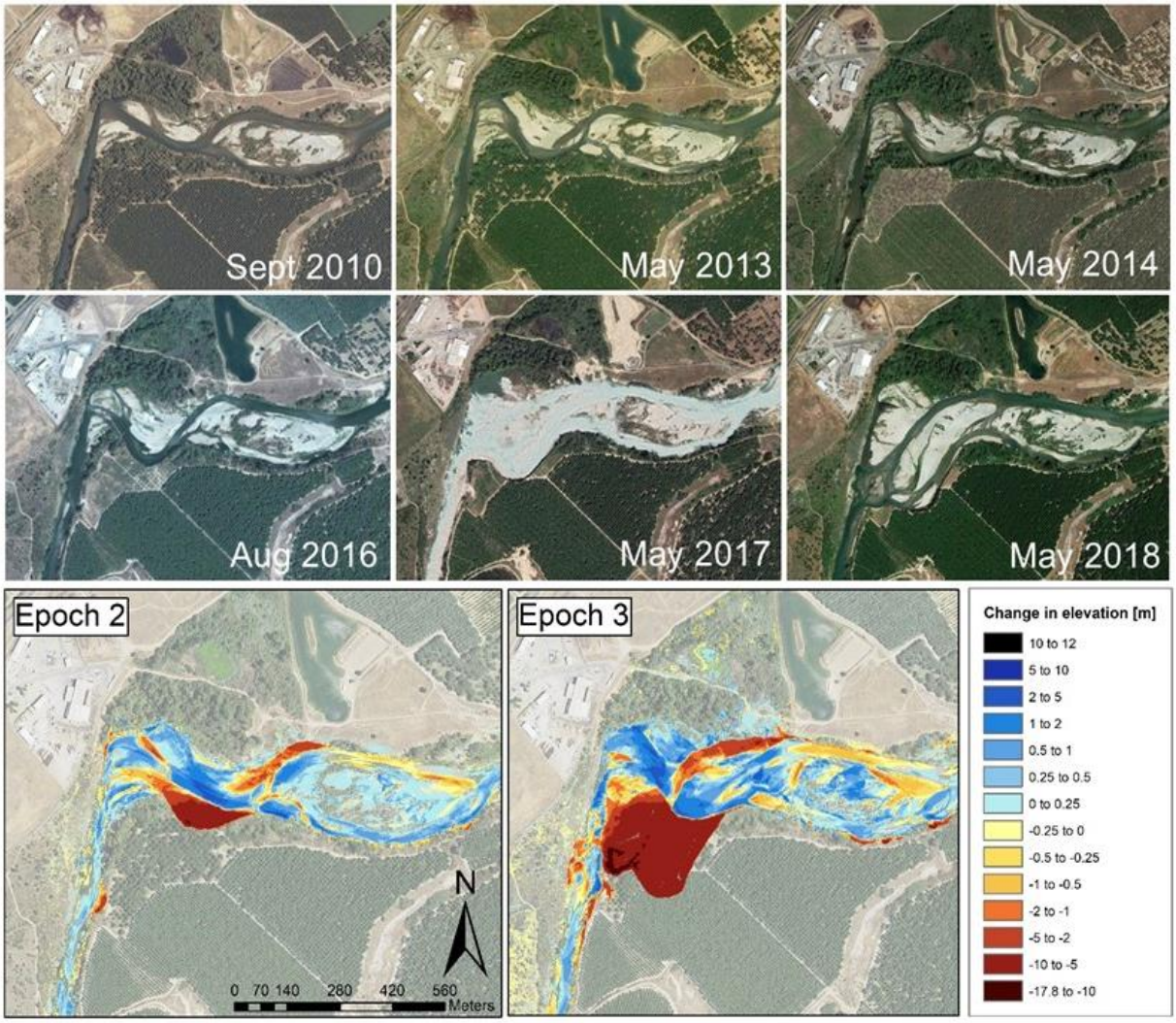

Figure 12. Top: HR terrace September 2010 – May 2018 (Google Earth Pro, 2020). Bottom: Epoch 2 and 3 DoD rasters.

6.2 Study Question 2: Hydrology and geomorphic response

Upon acknowledging the local topographic drivers at the reach scale and internal dynamism inherent in the LYR system due to historical and current impacts and influences, the hydrologic metrics offer further explanation of topographic changes observed at the segment scale across the study epochs. The hydrologic metrics yielded compelling evidence that a long duration flood, releasing sustained volumes of water above high inundation thresholds may cause more scour and net export, especially in a system such as the LYR where the channel is well-connected to its expansive floodplain, allowing access to erode those sediments.

6.2.1 Flood peak magnitude not correlated with erosion and export

The main finding of this study was that peak discharge was not correlated with total scour nor net export of sediment across epochs, and the contradictions were stark. Despite a flood peak during epoch 1 that was 1.5x greater than the peak of epoch 2, not only was there not 150% more sediment export–or any greater sediment export in epoch 1, but instead there was 33% more sediment exported during drought epoch 2 (**Figure 4**). Net export then increased to 1.37 x 10^6 m^3 over flood epoch 3, a 21.8x increase in export from the first flood epoch 1, even though epoch 3 had a 25% lower peak flood. Of the 1.57 x 10^6 m^3 net volume of sediment exported out of the LYR over the 18-year period, 87.2% occurred over 3 years during epoch 3 (**Figure 4**).

It is important to differentiate the statement “more erosion” as it relates to net scour/export versus total scour. The first indicates how well re-deposition balanced erosion, while the second captures the magnitude of scour events alone. Epoch 1 actually did experience much more total scour than epoch 2 (-2.52 x 10^6 m^3 and -0.64 x 10^6 m^3 respectively) (**Figure 5**). The key difference was that re-deposition in epoch 1 was great enough to nearly negate scour. Segment scale re-deposition was positively related to peak discharge which explains the small net export of epoch 1. In epoch 3, scour volume was greater than in epoch 1 by 34.7% while re-deposition decreased by 17%, causing a large overall increase in net export. A stronger relationship exists between total scour and the hydrologic duration and volume metrics, rather than the peak metric. Comparing total scour between the two flood epochs shows a connection between scour and volume discharged, especially above floodway stage (**Figure 9**, **Figure 13**).

Comparing the relationship between net and total scour and their respective flood peaks contrasts with uniform channel dynamics, where higher discharge leads to more erosion as dictated by total bed load transport. However, Yuba River hydro-geomorphic dynamism fits well within the geomorphic effectiveness framework and flood archetypes from the literature. The

epoch 3 period experienced long duration flooding and high volume released, especially above floodway, with the peak flood year (2017) experiencing the greatest annual volume of discharge, analogous to flood energy, relative to the previous two epochs (**Figure 9**, **Table 2**). While the epoch 1 flood best matches the type A flood curve, with a high peak and short duration, epoch 3 fits the profile for the type B high peak, long duration flood type as described by the geomorphic effectiveness model (**Figure 2**). Type B flood types are predicted to be the most geomorphically effective fluvial events in any landscape and include exceptional floods like the Rubicon River, California (1964) and Teton River, Idaho (1976) dam-failure floods, and colossal paleofloods like the Missoula Flood, Columbia River Gorge (~13,000 years before present) and the Bonneville Flood, Idaho (~14,500 years before present) (Costa and O' Connor, 1995).

These findings highlight why annual peak discharge, one of the most common hydrologic metrics used in flood frequency analysis, can be a simplified and problematic indicator of the true magnitude of a flood period in regard to fluvial geomorphic response. Although the traditional annual maximum method is still the most commonly used in many countries, defining samples using only this method results in a loss of information, and improvements to flood frequency analysis techniques to capture the behavior of extreme hydrological events are still sought after for this reason (Lang et al., 1999; Bačová-Mitková & Onderka, 2010). Ideally, methods account for temporal complexities of the regime—one example is the peaks-over-threshold (partial duration series) method (Lang et al., 1999) which accounts for years with multiple flood events. However, this still fails to capture both water volume and its temporal distribution; further, this must be translated into metrics at a scale significant to water management. This finding is significant because years with multiple flood peaks and sustained flooding (high annual volume) can stress reservoir infrastructure; indeed, these two characteristics were defining features of the 2017 water year which exacerbated

conditions during the Oroville emergency spillway failure (White et al., 2019; Vano et al., 2019) ~45 km north of the LYR on the Feather River.

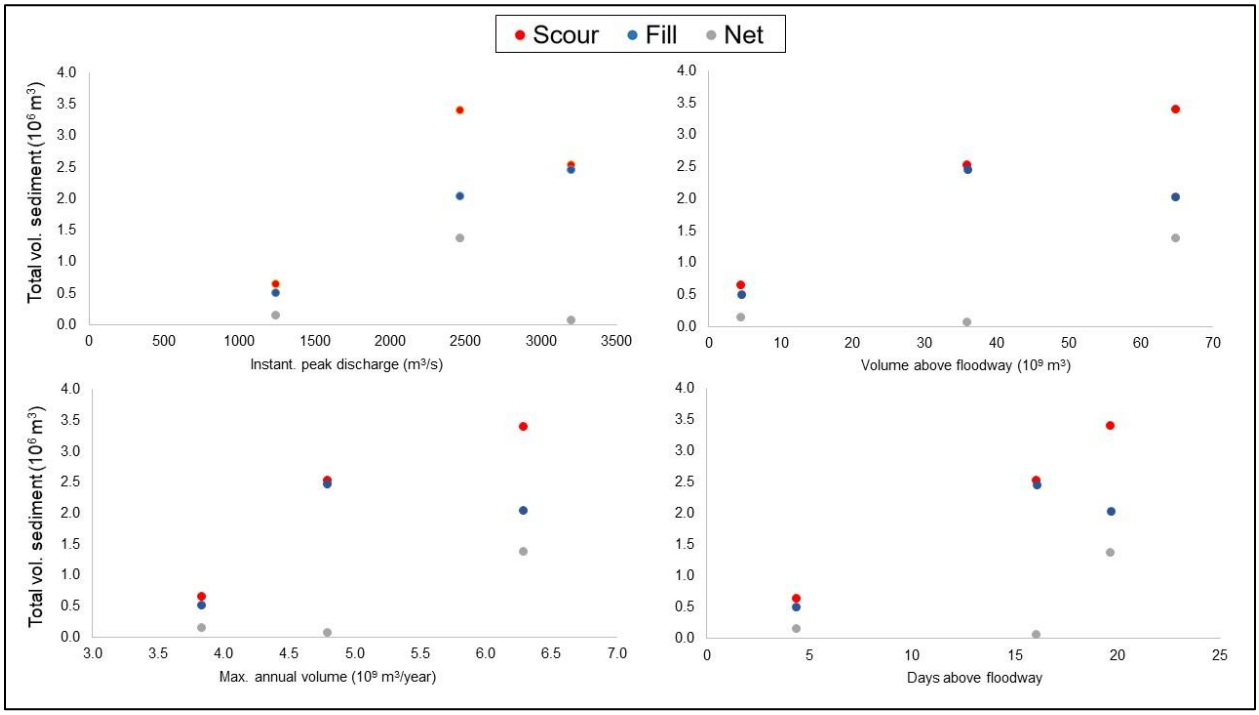

Figure 13. Example relationships between scour, fill, and net topographic change at the segment scale (y-axis) against various hydrologic metrics (x-axis).

6.2.2 In-channel vs overbank dynamics

The in-channel versus overbank dynamics help explain how topographic changes varied at two distinct inundation levels. Because overbank regions were always net scour, they explain the majority of the LYR's net export patterns across the study epochs. In epochs 1 and 3, 80% of scour was overbank scour (**Figure 5**) from terrain above an inundation level of 113.26 m^3/s. In epoch 1 the LYR experienced one high peak, short duration Winter flood pulse in the 2006 water year; the geomorphic response that allowed the LYR to remain nearly neutral in terms of net export was that sediment eroded upstream was then re-deposited in the overbank (as 1.84 x 10^6 m^3 of overbank fill), especially in reaches below DPD (**Figure 6**). Due to the nature of the multi-flood epoch 3 period, it is possible that the same overbank re-deposition process may

have initially resulted following the first flood pulse, with the subsequent sustained flood leading to evacuation of that re-deposited sediment. Interestingly, the in-channel region also experienced the most fill in epoch 3 (**Figure 5**) displaying how this geomorphically impactful flood period drastically changed the channel geometry. Indeed, areas that were initially overbank in 2014 but became in-channel in 2017 accounted for 62% of overbank scour, confirming lateral migration was a dominant scour process in epoch 3.

6.2.3 Effects of flow variability and antecedent conditions

Topographic change outcomes result from the interaction of topographic drivers and hydrology, but observed effects are dependent on time as a second-order variable. What is measured is a product of the time span of observation (e.g., **Figure 12**). Uniform channel dynamics equations dictate that higher flow leads to more erosion; Recking et al. (2012), however, noted that in field experiments, the predictive accuracy of erosional behavior using channel bed load transport equations increases over longer timescales of measurement. Further, Lisenby et al. (2016) caution against the notion of expecting geomorphic response to scale linearly with energy input, given the often non-linear behavior of complex river systems with diversity of topography, processes, and non-uniform flow patterns.

Arid environments experience extreme variability in discharge; large flood events are infrequent, separated by dry, low flow conditions (Gregory, 2006). Mediterranean climates, like this study area, are particularly prone to ‘whiplash’ events involving rapid shifts from extreme drought to extreme flood conditions, such as the 2016-2017 flood period following the dry 2012-2016 period in California (Swain et al., 2018). El Niño years experience above-normal precipitation concentrated in winter, generally resulting in landsliding and greater fluvial sediment flux (Mertes and Warrick, 2001; Gray et al., 2015b; East et al., 2018b). Drought periods can lead to decreased soil moisture, low runoff efficiency (Davenport et al., 2020), and a build-up of flood-transportable sediments. Therefore, the large sediment evacuation event

observed in epoch 3 may also be a product of the extremely dry conditions leading up to the event. The LYR's flow regime is quite dynamic, and flow heterogeneity is known to promote process diversity (Parker et al, 2003). It is pertinent, therefore, to also account for antecedent conditions, regime variability, and concentration of flow volume in time when predicting geomorphic response.

7 Conclusions

Morphodynamic processes in rivers are comprised of complex interactions between topography and hydrology. However, hydrographic forcing is independent in that hydrologic input is a driver external to the river system itself (**Figure 1**). Therefore, characterization and differentiation of hydrologic metrics is important in order to distinguish different flood period 'types' (e.g., types A, B, C of the geomorphic effectiveness flood energy model), and their effects. While the 'cause' and 'effect' aspect of fluvial geomorphology is hardly straightforward, it is nonetheless the goal of geomorphic effectiveness studies and fluvial morphodynamics models to link geomorphic pattern to hydrologic metric. This study presents a novel approach to distinguish flood periods at a scale significant to geomorphic river response, using threshold-based volume and duration analysis. Peak discharge was not found to be as important in explaining net export and total scour of sediment as duration and volume of flood events, highlighting the significance of inclusion of these hydrologic metrics in considerations for river infrastructure design, erosion control, and flood planning.

8 Acknowledgements

Primary support for this study was provided by the Yuba Water Agency [award # 201016094]. Additional support came from the USDA National Institute of Food and Agriculture, Hatch [project number CA-D-LAW-7034-H], and the Hydrologic Sciences Graduate Group at

University of California, Davis. I thank my advisor Greg Pasternack, for providing timely and exceptional guidance on this project, helping me to understand river processes and also encouraging my academic and personal growth. Additional acknowledgement goes to the members of the Pasternack lab, past and present, for providing an enormous foundation of topographic change work and DEM processing work that made this kind of long-term, large-scale perspective possible; I especially thank Jason Weiner, Paulo Silva, Jennifer Carley, Joshua Wyrick, Rocko Brown, and Matthew Weber whose work contributed directly to this project. I thank UC Davis professor Jonathan Herman, USGS geologist Amy East, and Geoff Rabone of the Yuba Water Agency for review of a draft of the manuscript. I thank the staff from Quantum Spatial for their help collecting and processing LiDAR data in 2014 and 2017. Lastly, I thank my mother Audrey Gervasi, who consistently encourages and supports my environmental science endeavors, and helped me to complete graduate school even in the midst of an unprecedented global pandemic.

9 References

Abu-Aly, T.R., Pasternack, G.B., Wyrick, J.R., Barker, R., Massa, D., Johnson, T., 2014. Effects of LiDAR-derived, spatially distributed vegetation roughness on two-dimensional hydraulics in a gravel–cobble river at flows of 0.2 to 20 times bankfull. Geomorphology 206, 468–482.

Adler, L.L., 1980. Adjustment of the Yuba River, California, to the Influx of Hydraulic Mining Debris, 1849–1979. Master of Arts, University of California, Los Angeles, p. 180.

Bačová-Mitková, V., Onderka, M., 2010. Analysis of extreme hydrological events on the Danube using the peak over threshold method. Journal of Hydrology and Hydromechanics 58(2), 88–101.

Bagnold, R.A., 1977. Bed load transport by natural rivers. Water Resources Research 13(2), 303–312.

Bezak, N., Brilly, M., Šraj, M., 2014. Comparison between the peaks-over-threshold method and the annual maximum method for flood frequency analysis. Hydrological Sciences Journal 59(5), 959-977.

Brown, A.G., Tooth, S., Bullard, J.E., Thomas, D.S.G., Chiverrell, R.C., Plater, A.J., Murton, J., Thorndycraft, V.R., Tarolli, P., Rose, J., Wainwright, J., Downs, P., Aalto, R., 2017. The

geomorphology of the Anthropocene: emergence, status and implications. Earth Surface Processes and Landforms 42, 71–90.

Carley, J.K., Pasternack, G.B., Wyrick, J.R., Barker, J.R., Bratovich, P.M., Massa, D.A., Johnson, T.R., 2012. Significant decadal channel change 58–67 years post-dam accounting for uncertainty in topographic change detection between contour maps and point cloud models. Geomorphology 179, 71–88.

Carling, P., 1988. The concept of dominant discharge applied to two gravel-bed streams in relation to channel stability thresholds. Earth Surface Processes and Landforms 13, 355–367.

Costa, J.E., O'Connor, J.E., 1995. Geomorphically effective floods. In: Costa, J.E., Miller, A.J., Potter, K.W., Wilcock, P.R. (Eds.), Natural and Anthropogenic Influences in Fluvial Geomorphology. American Geophysical Union, Washington, DC.

Davenport, F.V., Herrera-Estrada, J.E., Burke, M., Diffenbaugh, N.S., 2020. Flood size increases nonlinearly across the western United States in response to lower snow-precipitation ratios. Water Resources Research 56.

Dettinger, M., 2011. Climate change, atmospheric rivers, and floods in California-a multimodel analysis of storm frequency and magnitude changes. J. Am. Water Resour. Assoc. 47 (3), 514–523.

Dietrich, W.E., Kirchner, J.W., Ikeda, H., Iseya, F., 1989. Sediment supply and the development of the coarse surface layer in gravel-bedded rivers. Nature 340, 215–217.

Duboys, M.P., 1879. Etudes du Regime et l'Action Exerćee par les Eaux sur un Lit à Fond de Graviers Indefiniment Affouilable. Annates de Fonts et Chausses, 5(18), 141-195.

East, A.E., Logan, J.B., Mastin, M.C., Ritchie, A.C., Bountry, J.A., Magirl, C.S., Sankey, J.B., 2018a. Geomorphic evolution of a gravel-bed river under sediment-starved versus sediment-rich conditions: river response to the world’s largest dam removal. Journal of Geophysical Research: Earth Surface 123(12), 3338–3369.

East, A.E., Stevens, A.W., Ritchie, A.C., Barnard, P.L., Campbell-Swarzenski, P., Collins, B.D., Conaway, C.H., 2018b. A regime shift in sediment export from a coastal watershed during a record wet winter, California: Implications for landscape response to hydroclimatic extremes. Earth Surf. Process. Landforms 43, 2562–2577.

Gershunov, A., Shulgina, T., Ralph, F.M., Lavers, D.A., Rutz, J.J., 2017. Assessing the climate-scale variability of atmospheric rivers affecting western North America. Geophysical Research Letters 44, 7900–7908.

Gilbert, G.K., 1917. Hydraulic-mining debris in the Sierra Nevada. United States Geological Survey Professional Paper 105, Washington, D.C.

Google Earth Pro, v. 7.3.3.7786, 2020. Recology Yuba Sutter. 39° 9'50.52"N, 121°33'6.21"W. Accessed Oct. 2020.

Grant, G.E., Schmidt, J.C., Lewis, S.L., 2003. A geological framework for interpreting downstream effects of dams on rivers. In A Peculiar River, O’Connor JE, Grant GE (eds). American Geophysical Union: Washington, DC, 209–223.

Gray, A.B., Pasternack, G.B., Watson, E.B., Warrick, J.A., Goñi, M.A., 2015a. Effects of antecedent hydrologic conditions, time dependence, and climate cycles on the suspended sediment load of the Salinas River, California. Journal of Hydrology 525, 632-649.

Gray, A.B., Pasternack, G.B., Watson, E.B., Warrick, J.A., Goñi, M.A., 2015b. The effect of El Niño Southern Oscillation cycles on the decadal scale suspended sediment behavior of a coastal dry-summer subtropical catchment. Earth Surface Processes and Landforms 40, 272–284.

Gregory, K.J., 2006. The human role in changing river channels. Geomorphology 79(3–4), 172–191.

Guinn, J.M., 1890. Exceptional years: a history of California floods and drought. Hist. Soc. South. Calif. 5(1), 33–39.

James, L.A., 2005. Sediment from hydraulic mining detained by Englebright and small dams in the Yuba basin. Geomorphology 71, 202-226.

James, L.A., Singer, M.B., Ghoshal, S., Megison, M., 2009. Historical channel changes in the lower Yuba and Feather Rivers, California: long-term effects of contrasting river-management strategies. In: James, L.A., Rathburn, S.L., Whittecar, G.R. (Eds), Management and Restoration of Fluvial Systems with Broad Historical Changes and Human Impacts. Geological Society of America Special Paper 451, 57–81.

Kleinhans, M.G., 2010. Sorting out river channel patterns. Prog. Phys. Geogr. 34 (3), 287–326.

Kondolf, G.M., 1997. Hungry water: Effects of dams and gravel mining on river channels, Environ. Manage. 21(4), 533–551

Lancaster, S.T., Hayes, S.K., Grant, G.E., 2003: Effects of wood on debris flow runout in small mountain watersheds. Water Resources Research 39(6), EP1168.

Lane, E.W., 1955. The importance of fluvial morphology in hydraulic engineering. Proceedings of the American Society of Civil Engineers 81, 1–17.

Lang, M., Ouarda, T.B.M.J., Bobée, B., 1999. Towards operational guidelines for over-threshold modeling. Journal of Hydrology 225(3–4), 103–117.

Lenzi, M.A., Mao, L., Comiti, F., 2006. Effective discharge for sediment transport in a mountain river: computational approaches and geomorphic effectiveness. Journal of Hydrology 326, 257–276.

Lisenby, P.E., Croke, J., Fryirs, K.A., 2016. Geomorphic effectiveness: a linear concept in a non-linear world. Earth Surface Processes and Landforms 43(1), 4–20.

Mertes, L.A.K., Warrick, J.A., 2001. Measuring flood output from 110 coastal watersheds in California with field measurements and SeaWiFS. Geology 29, 659–662.

Montgomery, D.R., Buffington, J.M., 1997. Channel-reach morphology in mountain drainage basins. Geol. Soc. Am. Bull. 109, 596–611.

Parker, G., Toro-Escobar, C.M., Ramey, M., Beck, S., 2003. The effect of floodwater extraction on the morphology of mountain streams. Journal of Hydraulic Engineering 129(11), 885–895.

Pasternack, G.B., Wyrick, J. R., 2016. Flood-driven topographic changes in a gravel-cobble

river over segment, reach, and unit scales. Earth Surface Processes and Landforms, 42 (3): 487-502.

Pasternack, G.B., Baig, D., Weber, M.D., Brown, R.A., 2018. Hierarchically nested river landform sequences. Part 1: Theory. Earth Surface Processes and Landforms 43(12), 2510–2518.

Peckham, S.D., 2003: Fluvial landscape models and catchment-scale sediment transport. Global and Planetary Change 39, 31–51.

Pickup, G., 1976. Adjustment of stream-channel shape to hydrologic regime. J. Hydrol. 30, 365--373.

Poff, N.L., Allan, J.D., Bain, M.B., Karr, J.R., Prestegaard, K.L., Richter, B.D., Sparks, R.E., Stromberg, J.C., 1997. The natural flow regime: A paradigm for river conservation and restoration. BioScience 47, 769–784.

Ralph, F.M., Neiman, P.J., Wick, G.A., Gutman, S.I., Dettinger, M.D., Cayan, D.R., White, A.B., 2006. Flooding on California's Russian River: role of atmospheric rivers. Geophys. Res. Lett. 33, L13801.

Recking, A., Liébault, F., Peteuil, C., Jolimet, T., 2012. Testing bedload transport equations with consideration of time scales. Earth Surface Processes and Landforms 37(7), 774–789.

Swain, D.L., Langenbrunner, B., Neelin, J.D., Hall, A., 2018. Increasing precipitation volatility in twenty-first-century California. Nature Climate Change 8, 427–433.

Vano, J.A., Dettinger, M.D., Cifelli, R., Curtis, D., Dufour, A., Miller, K., Olsen, J.R., Wilson, A.M., 2019. Hydroclimatic extremes as challenges for the water management community: Lessons from Oroville Dam and Hurricane Harvey. Bull. Amer. Meteor. Soc. 100 (1), S9–S14.

Weber, M.D., Pasternack, G.B., 2017. Valley-scale morphology drives differences in fluvial sediment budgets and incision rates during contrasting flow regimes. Geomorphology 288, 39-51.

White, A.B., Moore, B.J., Gottas, D.J., Neiman, P.J., 2019. Winter storm conditions leading to excessive runoff above California’s Oroville dam during January and February 2017. Bull. Amer. Meteor. Soc. 100, 55–70.

Williams, G.P., Wolman, M.G., 1984. Downstream Effects of Dams on Alluvial Rivers. Professional Paper, 1286. U.S. Geological Survey, Washington, DC.

Wolman, M.G., Miller, J.P., 1960. Magnitude and frequency of forces in geomorphic processes. J. Geol. 68, 54-74.

Wyrick, J.R., Pasternack, G.B., 2012. Landforms of the Lower Yuba River. University of California, Davis, CA.

Wyrick, J.R., Pasternack, G.B., 2015. Revealing the natural complexity of topographic change processes through repeat surveys and decision-tree classification. Earth Surface Processes and Landforms, 41 (6) 723-737.

Yochum, S.E., Sholtes, J.S., Scott, J.A., Bledsoe, B.P., 2017. Stream power framework for predicting geomorphic change: The 2013 Colorado Front Range flood. Geomorphology 292, 178–192.